https://doi.org/10.17221/56/2020-JFS

Satellite image processing of the Buxus hyrcana Pojark dieback in the Northern Forests of Iran

Marzieh Ghavidel[1], Peyman Bayat[1]*, Mohammad Ebrahim Farashiani[2]*

[1]Department of Computer, Faculty of Engineering, Rasht Branch, Islamic Azad University, Rasht, Iran
[2]Research Institute of Plant Protection, Agricultural Research, Education and Extension Organization, Tehran, Iran

**Corresponding authors: ghavidel@iau.ac.ir; Bayat@iaurasht.ac.ir*

Citation: Ghavidel M., Bayat P., Farashiani M.E. (2021): Satellite image processing of the Buxus hyrcana Pojark dieback in the Northern Forests of Iran. J. For. Sci., 67: 71–79.

Abstract: Pests and diseases can cause a variety of reactions in plants. In recent years, the boxwood dieback has become one of the essential concerns of practitioners and natural resources managers in Iran. To control the boxwood dieback spread, the early detection and disease distribution maps are required. The boxwood dieback causes a range of changes in colour, shape and leaf size with respect to photosynthesis and transpiration. Through remote sensing techniques, e.g. satellite image processing data, the variation of thermal and visual characteristics of the plant could be used to measure and illustrate the symptoms of the disease. In this study, five common vegetation indices like difference vegetation index (DVI), normalized difference vegetation index (NDVI), soil adjusted vegetation index (SAVI), simple ratio (SR), and plant health index (PHI) were extracted and calculated from Landsat 8 satellite image data from six regions in the Gilan province, located in the northern part of Iran out of 150 maps over the time period 2014–2018. It turned out that among the aforementioned indices, based upon the results of the models, SR and NDVI indices were more useful for the disease spread, respectively. Our disease progression model fitting criteria showed that this technique could probably be used to assess the extent of the affected areas and also the disease progression in the investigated regions in future.

Keywords: image processing; vegetation indices; Landsat 8; forest; remote sensing

The crucial importance of forests in today's world no longer lies in their economic values but in their irreplaceable environmental benefits. The preservation of biodiversity is becoming one of the most critical issues in sustainable forest management (Ito et al. 2004). *Buxus hyrcana* Pojark is one of the few evergreen broadleaved trees in Caspian forests with high longevity (Mohajer 2006) and is considered one of the Euxino-Hyrcanian elements (Boobak 1994). Although this species is referred to as a *Buxus sempervirens* L. provenance (Sabety 1994), it is different from its equivalent European species due to botanical and geographical differences. *Buxus hyrcana* Pojark has been introduced as a distinct plant taxon in the International Plant Names Index (IPNI) and is specific to Caspian forests (Esmaeilzadeh 2012). The best habitat for boxwood trees is located in northern Iran at 20–400 m a.s.l., but it is also seen up to a height of 1 200 m a.s.l. (Sabety 1994). The *Cydalima perspectalis* (box tree moth) is an invasive species on box tree *Buxus* spp. in Europe, which has been spreading and establishing across the continent during the last decade (Strachinis et al. 2015). In Iran, this disease has rapidly spread from west to east throughout the Hyrcanian boxwood stands and approximately 40 000 ha of the original boxwood stands were infested and damaged by this disease at different intensities (Esmaili et al. 2020). *Cydalima perspectalis* larvae feed on the leaves of different species of *Buxus*, seriously damaging these ornamental plants in private and public gardens as well as in semi-natural box-tree

https://doi.org/10.17221/56/2020-JFS

forests. In addition to the leaves, the larvae can attack the tree bark, causing the trees to dry out and die (Bella 2013). In recent years, boxwood blight has invaded and endangered one of the essential evergreen species in the Hirkani vegetation forests. The blight disease initially appears as irregular pale green watery spots mostly near the tip and the margin of the leaf. These spots grow rapidly into large brown and necrotic spots. If the condition for the continuation of the disease is desirable, the whole product will appear black and may disappear within a week (Ray et al. 2011). Because plant pathogens usually occur at significant levels, researchers are trying to use methods that are the basis of the landscape to evaluate and model the distribution of the disease and identify the effective factors and identify their interactions (Liu et al. 2007). The implementation of non-contact, highly efficient, and affordable methods for detecting and monitoring plant diseases and pests over vast areas could greatly facilitate plant protection. In this respect, different forms of remote sensing methods, e.g. satellite image based tools, have been introduced for detecting and monitoring plant diseases and pests in many ways (Zhang et al. 2019). When diseases and physiological stresses directly affect the reflectance properties of individual leaves, the most significant initial changes due to the sensitivity of chlorophyll to physiological disturbances often occur in the visible spectral regions of the infrared (Knipling 1970). It is shown that the reflectance beyond the spectrum (narrowband) is very important in determining the biophysical properties of crops (Ray et al. 2006).

Image processing methods are divided into two important categories. The first is the traditional/classical pixel-based one, employing an image pixel as a fundamental unit of the analysis. The second group is the object-based method, emphasizing, first, creating image objects and then using them for further analysis (Hussain et al. 2013). Object-based change detection is accomplished by comparing objects extracted from a new image with objects recorded in the site model (Hazel 2001). This classification involves the segmentation of an image into homogeneous objects followed by the analysis and classification of these objects (Whiteside et al. 2011). Vegetation index construction is one of the pixel-based techniques used in remote sensing image processing. There is considerable interest in utilizing remote sensing to estimate forest biophysical properties that are otherwise difficult to sample in the field. Several comprehensive reviews on the use of vegetation indices to assess ecological properties are found in many researches (Kerr and Ostrovsky 2003; Baloloy et al. 2018). In this study, for the first time, we use different plant vegetation indices based on Landsat 8 satellite imagery in six rural districts of the Gilan Province to detect unhealthy boxwood and also to come up with a predictive disease progression model of the *Buxus hyrcana* Pojark dieback disease spread across these rural districts. This is the first time that this sort of study is reported for this disease in the Gilan Province and maybe in Iran as a whole.

MATERIAL AND METHODS

In this study, six districts or areas of the Gilan Province were selected to evaluate the progress of *Buxus* destruction due to boxwood blight and to estimate contaminated regions. The reason for choosing these areas was that they had ground data for comparison. The areas of study were: Khaleh Sara Rural District, Talesh County, Asalem District; Khoshabar Rural District in the central part of Rezvanshahr city; Lavandvil Rural District, Lavandvil District, Astara County; Oshiyan, Chaboksar District, Rudsar County; Siahkalrud Rural District, Chaboksar District, Rudsar County; Virmuni Rural District in the central part of Astara County. These districts are shown in Figure 1.

In general, in order to access vegetation information, it is possible to combine at least two bands in satellite images and create a composite index called vegetation index. Vegetation indices are widely used as criteria for analysing land cover changes including vegetation and other factors (Kazeminia 2018). In this study, according to the necessity of studying the vegetation cover for determining the contamination status of the studied areas, the following indices difference vegetation index (DVI), normalized difference vegetation index (NDVI), soil adjusted vegetation index (SAVI), simple ratio (SR), and plant health index (PHI) were used. Table 1 gives the general explanation of these indices. These indices have their own biologically motivated definitions, for example NDVI for a given pixel always results in a number that ranges from −1 to +1; in which no green leaves give a value close to zero. A zero means no vegetation, however a high NDVI value, +1 (0.8–0.9) indicates healthy

https://doi.org/10.17221/56/2020-JFS

vegetation and a low NDVI value, –1 indicates less or no vegetation. These indices would help to develop a method for measuring plants in different conditions. Nowadays, many different vegetation indices have been developed. An Index-Data-Base, i.e. https://www.indexdatabase.de/, could be useful. According to the objectives of the study we aim to use spectral indices for detection of contaminated areas and to distinguish them from healthy ones. In this way, a wide range of different wavelengths would be useful for diagnosing the plant disease, as shown in Table 2. These wavelengths can be processed, and new indices could be measured.

In this study, to prepare satellite images from regions covered, the Earth Explorer (https://earthexplorer.usgs.gov/) and the images taken from Landsat 8 satellite with a spatial resolution of less than 30 m were used. The only limitation of these images is the temporal resolution of the Landsat 8 satellite that slightly decreases the accuracy of the index estimation. In this study, images taken from 2014 to 2018 in the range of rural districts in mid-January each year were used. It is reported that with the transformation of grey to high atmosphere reflectance, the quality level for water and soil classification could be promoted dramatically (Maglione et al. 2013). In this study, the radiometric detection of the Landsat 8 satellite was performed by converting the grey level of each image pixel to high atmosphere reflectance values using metadata. To determine the mean value of each index at the province level, the histogram was used. Also, the area for each class was calculated using pixel number multiplication. Finally, we used the ArcMap software (https://desktop.arcgis.com/en/arcmap/) to get the job done.

RESULTS AND DISCUSSION

For each vegetation index, 30 output maps (in total 150 maps) were extracted. To conform to the allowable number of paper pages here, only the NDVI index output maps of six districts (2018) are reported. To validate the calculated vegetation indices the field data on the vegetation status in six areas was used. The output maps of the NDVI indexing in 2018 are shown in Figure 2.

Again, due to the paper size limitation, only the field data of Lavandvil district are used for analysis. In Lavandvil, eleven polygons were monitored whose names and geographical coordinates are listed in Table 3.

Table 4 summarizes the results of field surveys and the results of indices obtained in satellite images in the target polygons. The root mean square error

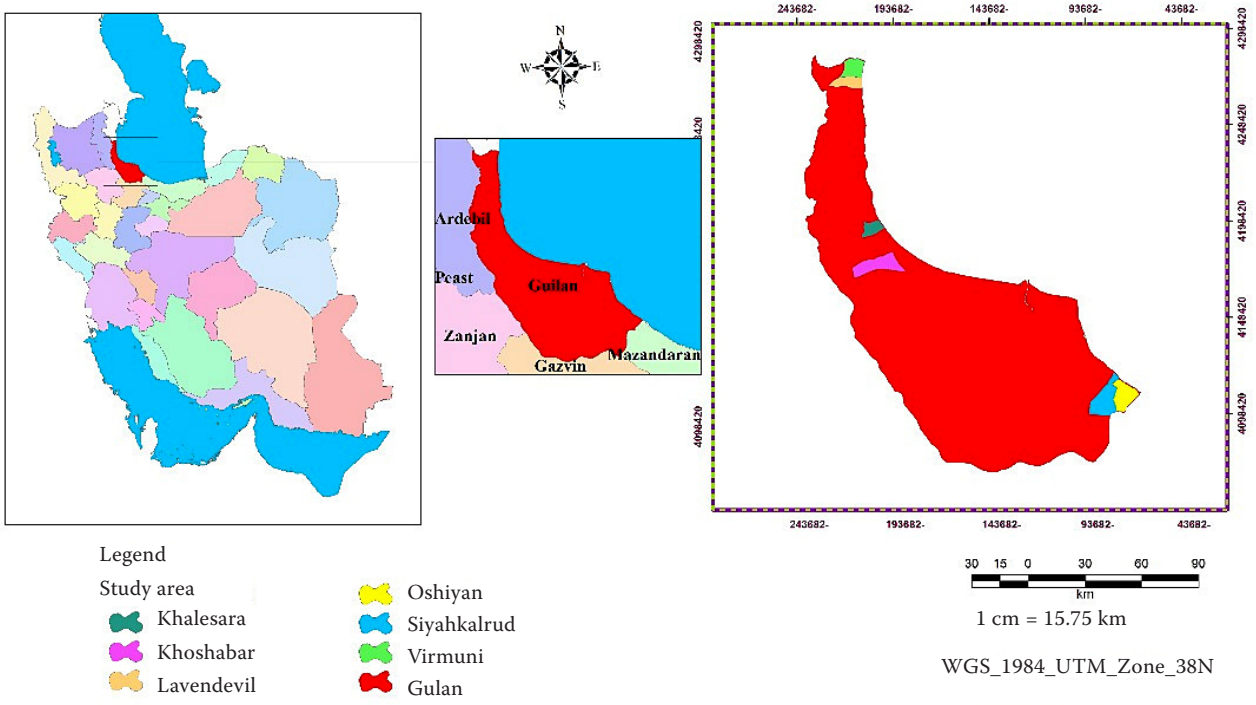

Figure 1. The geographical location of the studied rural districts in Gilan province

https://doi.org/10.17221/56/2020-JFS

Table 1. The general explanation applied to vegetation indices

Index	Explanation	Equation
DVI	The difference vegetation index is used to distinguish between soil and vegetation; however, it does not take into account the effect of atmosphere reflectance or shadows (Naji 2018). The DVI index ranges from 1 to 0 for marine and non-vegetated areas and from 0 to 0.07 for unhealthy vegetation and from 0.07 to higher value (often 1) for areas with healthy plants (Vani, Mandla 2017).	NIR-R
NDVI	The normalized difference index vegetation indicates how many green leaves exist. NDVI is calculated using the measured light intensity only at two wavelengths, e.g., near-infrared (NIR, 780-890 nm) and red (R, 650–680 nm) using (NIR+R)/(NIR-R) equation (Robinson et al. 2017). The NDVI index ranges for aquatic or non-vegetated areas (mountains or boulders) from –1 to 0, for areas with unhealthy or contaminated vegetation from 0 to 0.33 and for areas with healthy plants from 0.33 up to 1 (GISGeography 2019). However, it should be noted that the magnitude of changes in this index for both healthy and unhealthy vegetation areas can be reduced by 0.1% in the cold season due to lower image contrast and in the hot season it should be increased by 0.1 due to higher image contrast.	(NIR-R)/ (NIR+R)
SAVI	The soil-adjusted vegetation index is one of the most common indices that is only slightly different from the NDVI index. The difference lies in a factor that can be used to moderate the effect of background soil. The NDVI index is affected by soil reflectance in some areas. It overshadows the recorded reflectance for vegetation. SAVI index solves this problem in the NDVI index. This index uses a factor called L to moderate the effect of background soil. The value of this parameter is a function of the amount of vegetation available in the area and prior knowledge the user has of the vegetation density status in the area and is calculated using (1+L){(NIR-R)(NIR+R+L) equation (Garcia, Perez 2016). The amplitude of changes in the SAVI index for aquatic and non-vegetated areas is the same as for the NDVI index from 1 to 0, for areas with unhealthy vegetation from 0 to 0.15 and for areas with healthy vegetation from 0.15 to 1; by the way, L factor is set at 0.5 (Vani, Mandla 2017). This parameter reduces the field-effect index and reflects a lower plant cover percentage.	(R+L)/(NIR-)/ NIR+R+L)
SR	The solar reflectivity is composed of a simple ratio between two bands, one with the highest and the other with the lowest reflectance concerning vegetation. This index is calculated using the (NIR/R) equation (Melillos, Hadjimitsis 2020). The range of SR index variations for aquatic and non-vegetated zones is from 1 to 1, for regions with unhealthy vegetation from 1 to 2.2 and for regions with healthy plants from 2.2 to higher values (Robinson et al. 2017)	(NIR/R)
PHI	The plant health instructor index is also used to determine the health condition of the plants in some regions and can be calculated using the equation 1.4 × LN(DVI) + 1.298. This index is mostly used to identify the health status and the regions of water without vegetation. The amplitude of changes in the PHI index for aquatic and vegetation-free regions is pixel-free. It is shown as NaN, for the unhealthy vegetation from -n to -18 and for the regions with healthy vegetation from –8 to –0 (Asadi et al. 2016).	1.4 × LN(DVI) + +1.298

DVI – difference vegetation index; NDVI – normalized difference vegetation index; SAVI – soil adjusted vegetation index; SR – simple ratio; PHI – plant health index

(RMSE) and the root of the mean squared normal error (NRMSE) were used to measure the accuracy of the model in predicting the contaminated area.

The total hectares for evaluated contaminated area by the index (ECA) and observed contaminated area (OCA) were 34.55 and 31.24, respectively. Also, RMSE and NRMSE were 2.90 and 9%, respectively. Given the RMSE and NRMSE values, the intensity of contamination observed and evaluated by the NDVI index was in full agreement with the estimates of the size of contaminated areas in the specified polygons. It was not possible to compare the results of evaluating a complete polygon in the contaminated area of Lavandvil since the field data was not fully available due to inaccessibility of measuring data. The result is shown in Figure 1. In this graph, the percentage of unhealthy pixels is calculated by summing the pixels at the above time intervals. Without deep explanation, the calculated indices and their profiles are given in Table 5 and Figure 3. Table 5 also summarizes

https://doi.org/10.17221/56/2020-JFS

Table 2. Comparison of the thermal and visual features representing the diseased and healthy vegetation

Wavelength (nm)	Recognition capability
Visible (400–700)	The reflectance at the surface of diseased vegetation, especially in chlorophyll absorption bands, is increased due to the loss of chlorophyll and the presence of surface spores or mycelium.
Near-infrared (NIR) (700–1 200)	The red edge changes from 730 nm at the surface of healthy shadings to shorter wavelengths (e.g., 670 nm) at the diseased shading surface. Moreover, the reflectance at the surface of the diseased shadings is reduced due to aging and defoliation of the plant.
Thermal infrared band (TIR) (around 8 000–14 000)	The leaf temperature is increased by the reduction of transpiration due to root diseases and other diseases that cause the closure of the apertures in the early stages. Areas of the leaves that become watery because of cellular degradation can be colder at the beginning of the day or warmer at the end of the day, as the temperature of these leaves varies faster than in other leaves due to ambient conditions.

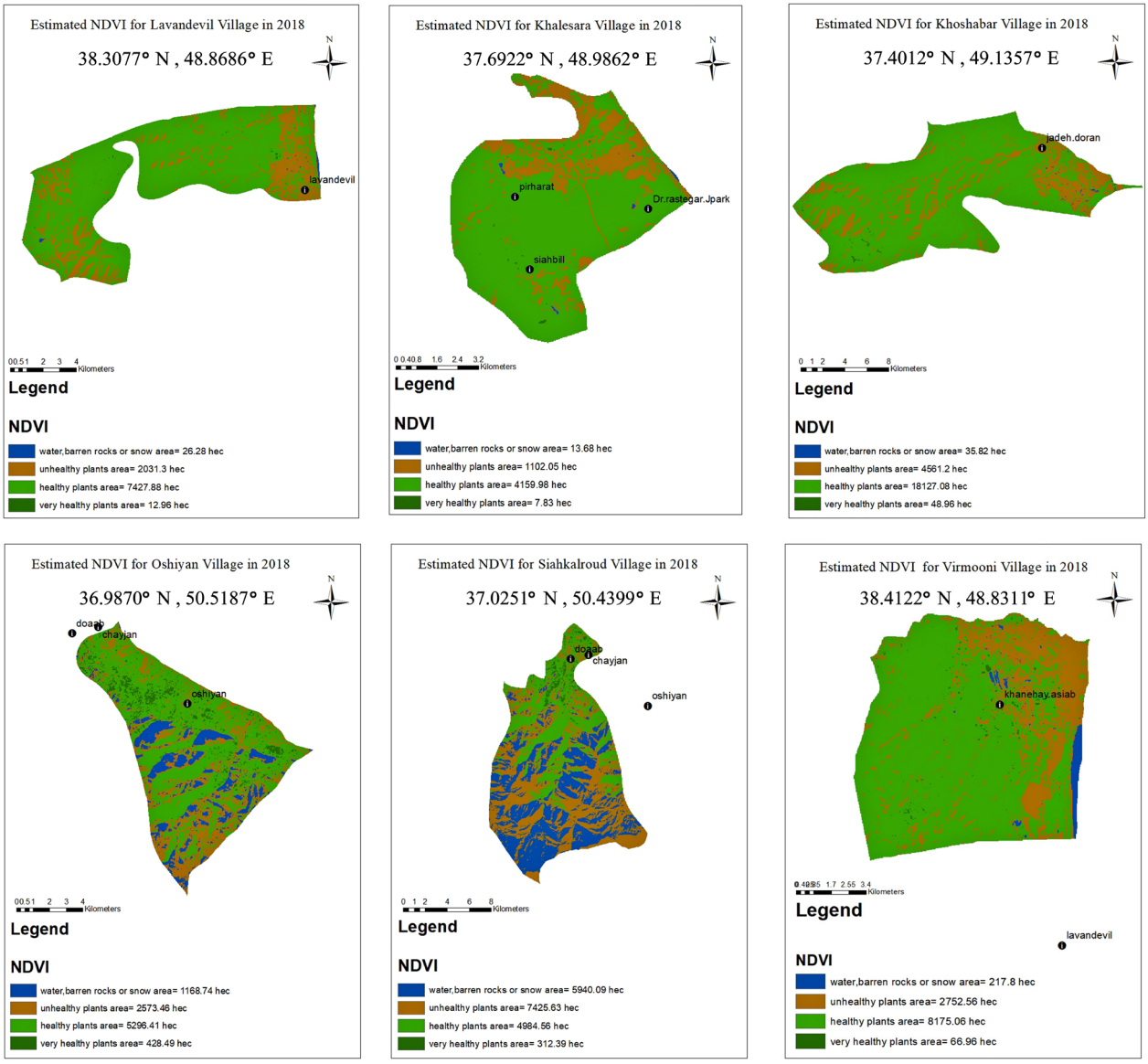

Figure 2. Output maps derived from normalized difference vegetation index (NDVI) indexing in 2018

https://doi.org/10.17221/56/2020-JFS

Table 3. Geographical coordinates of the monitored polygons in Lavandvil district

Geographical coordinates (UTM)	Elevation (m a.s.l.)	Habitat area (ha)	Region
313313, 4239269	17	2.5	Chelavand-Poshte Mahalleh
309877, 4239849	83	2.04	Lavandvil-Dashteh Kesh and Nazar Mahalleh
308666, 4239948	120	13.48	Lavandvil-Nazar Mahalleh
306984, 4240511	176	0.9	Lavandvil-Big Chelavand
304825, 4240040	385	2.06	Lavandvil-Shiri Hayati
304629, 4239557	273	1.01	Lavandvil-Shiri Hayati
304656, 4239783	319	0.15	Lavandvil-Shiri Hayati
312235, 4239445	27	0.15	Lavandvil-Chelavand-Hokm Darreh
311944, 242230	–2	0.19	Lavandvil-Kut Komeh
306456, 4242115	152	0.33	Lavandvil- Kut Komeh – Abe Garm
308423, 4244573	137	10.23	Lavandvil- Kanrud

the results of the indices applied to the images obtained from Lavandvil Village and the model estimation of unhealthy pixels in the region over the time period 2014–2018.

As can be seen, among the indices in the table, two indices SR and NDVI concerning the higher coefficient of explanation show a better feedback in estimating the model and forecasts of the status of pollution progression. On the other hand, although in most studies NDVI is considered as one of the best indices in vegetation, in the present study SR index shows better performance. It can be used for the diagnosis of healthy and unhealthy plants.

Due to the importance of Caspian boxwood and its high value in terms of biodiversity, it is very important to study the spatial distribution of boxwood blight disease and disease progression in different regions. Figure 3 shows the strong negative quadratic component to this bivariate relationship across all regions. It is to note that while the R^2 for each model is almost the same, the β coefficients of models from different regions are not the same. We should take into account that the multiple regression coefficients are supposed to reflect the predictor contribution of each variable to the model after controlling for collinearity among the predictors. The βs from the model using the centred-

Table 4. Comparison of contaminated regions by observation and evaluation methods

No.	Parts	ECA (ha)	ECI	OCA (ha)	OCI	Geographical coordinates (UTM)	
1	polygon 1	2.1	high	2.5	high	313313	4239269
2	polygon 2	3.78	high	2.04	high	309877	4239849
3	polygon 3	5.03	high	13.48	high	308666	4239948
4	polygon 4	0.4	high	0.9	high	306984	4240511
5	polygon 5	1.5	average	1	average	304825	4240040
6	polygon 6	0.9	average	0.5	average	304629	4239557
7	polygon 7	0.8	average	0.1	average	304656	4239783
8	polygon 8	0.42	high	0.15	high	312235	4239445
9	polygon 9	0.23	high	0.19	high	311944	4242230
10	polygon 10	0.02	average	0.15	average	306456	4242115
11	polygon 11	13.37	high	10.23	high	308423	4244573

ECA – evaluated contaminated area by the index; ECI – evaluated contaminated intensity; OCA – observed contaminated area; OCI – observed contamination intensity

https://doi.org/10.17221/56/2020-JFS

Table 5 Indexing results and the resulting prediction model

Index	Model	R^2	RMSE	NRMSE (%)
NDVI	$y = 0.0009x^3 - 0.0241x^2 - 3.8438x + 140.17$	0.95	2.90	9
DVI	$y = 3.6056x^3 - 319.86x^2 + 6\,384.5x + 33\,995$	0.89	4.57	15
SR	$y = 0.4814x^3 - 12.366x^2 - 2\,711.4x + 112\,310$	0.96	3.17	7
SAVI	$y = 0.5728x^3 + 119.55x^2 - 6\,666.7x + 136\,493$	0.70	5.22	14
PHI	$y = 1.912x^3 - 148.75x^2 + 1\,209.3x + 74\,572$	0.87	5.70	15

NDVI – normalized difference vegetation index; DVI – difference vegetation index; SR – simple ratio; SAVI – soil adjusted vegetation index; PHI – plant health index; RMSE – root mean square error; NRMSE – root of the mean squared normal error

squared term could clear the contribution of both linear and quadratic terms of the model. So, these discrepancies could be due to collinearity among the computed predictors and the need of model amendment. At the present time and likely in the past years, according to the results obtained in this study, the relationship between disease progression and geographical coordinates of areas would show

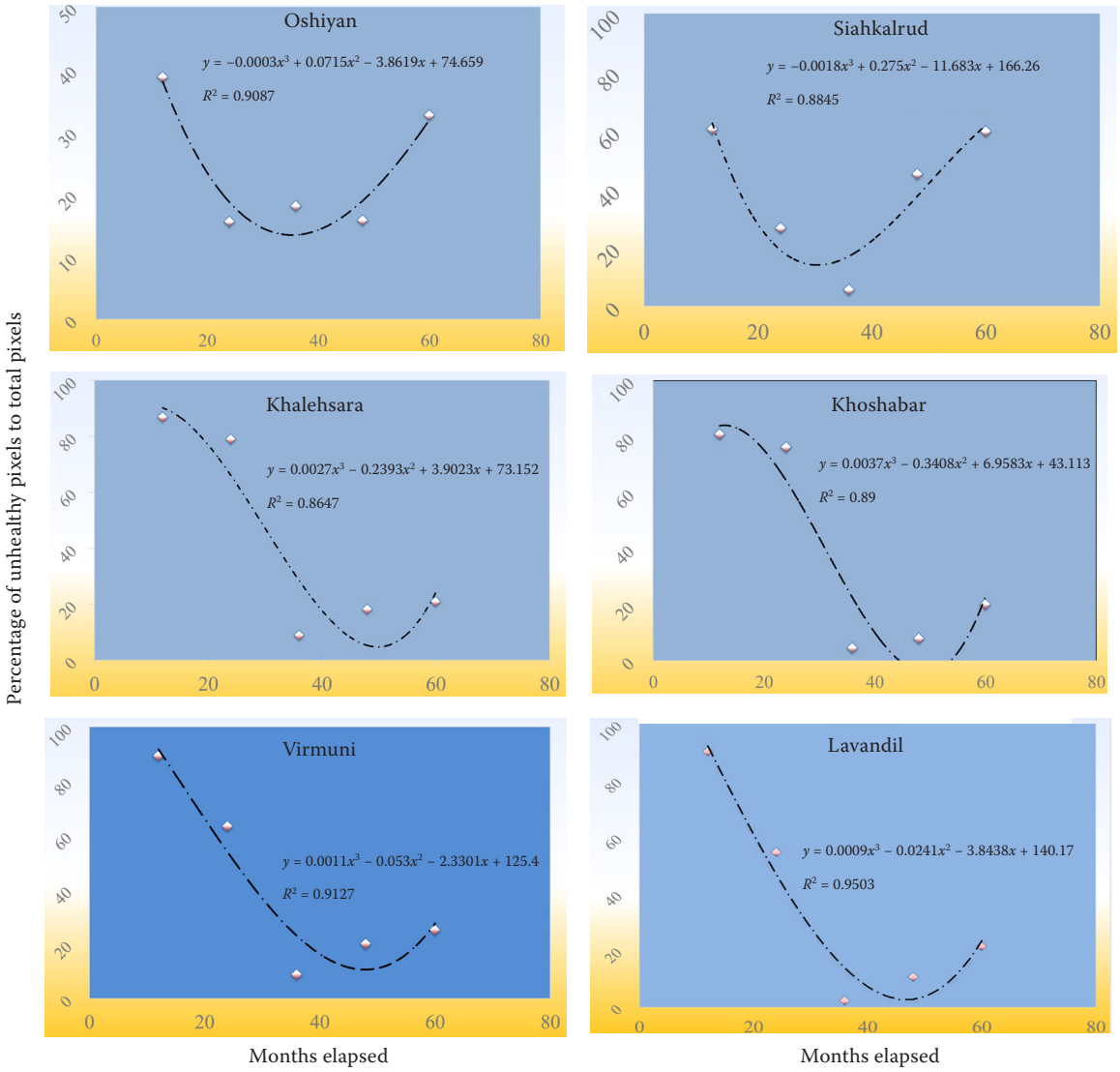

Figure 3. The course of disease progression during the year of survey in individual rural districts

https://doi.org/10.17221/56/2020-JFS

that the rate of disease progression in northern geographical coordinates was higher than it could be due to higher humidity and lower temperature. Obviously, in order to achieve closer and larger-scale results in the Gilan Province, it is necessary to first extract the distribution of boxwoods in the Gilan Province in the form of polygons with field visiting and then extract the equivalent polygons by satellite images to evaluate the unhealthy results of boxwood plants. Thus, in the coming years, instead of repeating field visits which require a lot of time and money, extracting images could be a reliable alternative tool. It should be noted that among the vegetation indices used in this study, SR index due to its capability to report the number of unhealthy pixels in the regions and its highest compliance with cardinal directions showed better performance. On the other hand, this index almost covers up other vegetation indices, so it can be considered for future evaluations. Remote sensing is a new tool for forest management, especially in large areas, which also has acceptable accuracy. In the present study, the use of plant indices in images obtained from the Landsat 8 satellite in several rural areas of the Gilan Province showed that these indices can be used to detect unhealthy vegetation and obtain a model of changes over the course of years.

In general, the characteristics of each habitat are affected by environmental, physiographical, altitude factors and slope aspect. Research has shown that combining environmental stresses with abiotic factors causes weakening, leaf fall, and tree decline (Lantschner, Corley 2015). Fungi are organisms that need environmental conditions to be present in an area. Nepstad et al. (2007), who mapped the pest-induced dead trees in the rainforests of Queensland, noted that cardinal direction was the main factor in the distribution of dead trees. Menge et al. (2013) investigated the effect of environmental factors including temperature, light and pH on the activity of blight fungi in *Anacardium occidentale*. One of the effective factors in controlling the activity of this fungus is that they have to spend a period of life in the dark (Menge et al. 2013). According to the results obtained from the vegetation indices, the highest percentage of unhealthy open pixels was in Vermoni, Lundville, Khalesara, Khoshabar, Siahkroud and Oshian regions. The results of this study are consistent with the results of research by Nespstad et al. (2007), who stated that the cardinal direction is correlated with the distribution and decay caused by fungi. Also, the obtained results from the vegetation indices in this study are in line with the results of Esmaili et al. (2016), who showed the distribution of boxwood blight disease and its relationship with some environmental factors in the Khibus boxwood forest. Esmaili et al. (2016) showed that drought conditions jeopardize the boxwood burn disease in the southern and southwestern directions and therefore, it could be seen as a controlling factor in the development and distribution of boxwood burn disease (Esmaili et al. 2016). This also explains the declining course of the disease in some years in the diagrams presented in Figure 3 with the improvement of vegetative conditions, but the activity of fungi and the progression of the disease increased again.

CONCLUSION

In this study, the use of vegetation indices on Landsat satellite 8 images in several rural districts of the Gilan Province showed that these indices could be used to detect unhealthy vegetation and obtain a model of changes over the desired years. Among these indices, according to the results of the models, SR and NDVI indices are more useful for healthy unhealthy trees, respectively. Obviously, to achieve closer and large-scale results at the Gilan Province level, it is necessary to extract the distribution of boxwoods in the Gilan Province in the form of polygons derived by field studies and surveys. The satellite image data provided similar results of polygons showing field visiting data. Thus, instead of repeating field visits that require a lot of time and expenses in the coming years, one could evaluate the image-based data. However, the satellite image data analysis of parallel polygons could precisely evaluate the unhealthy condition of boxwood plants.

REFERENCES

Asadi H., Esmailzadeh O., Hosseini S.M., Asri Y., Zare H. (2016): Application of cocktail method in vegetation classification. Journal of Taxonomy and Biosystematics, 8: 21–38.

Baloloy A.B., Blanco A.C., Candido C.G., Argamosa R J.L, Dumalag J.B.L.C., Dimapilis L.L.C., Paringit E.C. (2018): Estimation of mangrove forest aboveground biomass using multispectral bands, vegetation indices and biophysical variables derived from optical satellite imageries: rapideye, planetscope and sentinel-2. ISPRS Annals of Photogrammetry, Remote Sensing & Spatial Information Sciences, 4: 29–36.

https://doi.org/10.17221/56/2020-JFS

Bella S. (2013): The box tree moth *Cydalima perspectalis* (Walker, 1859) continues to spread in southern Europe: new records for Italy (Lepidoptera Pyraloidea Crambidae). Redia, 96: 51–55.

Boobak H. (1994). Natural Forests and Woody Plants of Iran Forests and Rangelands. Teheran, Research Institute of Forests and Rangelands.

Esmaeilzadeh O., Asadi H., Ahmadi A. (2012): Phytosociology of Khybus Protected Area. Journal of Wood and Forest Science and Technology, 19: 1–20.

Esmaili R., Soosani J., Shataee J.S., Naghavi H., Poorshakori F. (2016): Spatial distribution of buxus blight and its relation with some environmental factors (Case study: Khiboos Anjilsi protected area). Journal of Wood and Forest Science and Technology, 23: 147–167.

Esmaili R., Jouibary S.S., Soosani J., Naghavi H. (2020): Mapping of understory infested boxwood trees using high resolution imagery. Remote Sensing Applications: Society and Environment, 18: 100289.

Garcia P., Perez E. (2016): Mapping of soil sealing by vegetation indexes and built-up index: A case study in Madrid (Spain). Geoderma, 268: 100–107.

GISGeography (2019): What is NDVI (Normalized Difference Vegetation Index). Available at: https://gisgeography.com/ndvi-normalized-difference-vegetation-index/

Hazel G.G. (2001). Object-level change detection in spectral imagery. IEEE Transactions on Geoscience and Remote Sensing, 39: 553–561.

Hussain M., Chen D., Cheng A., Wei H., Stanley D. (2013): Change detection from remotely sensed images: From pixel-based to object-based approaches. ISPRS Journal of Photogrammetry and Remote Sensing, 80: 91–106.

Ito S., Nakayama R., Buckley G.P. (2004): Effects of previous land-use on plant species diversity in semi-natural and plantation forests in a warm-temperate region in Southeastern Kyushu, Japan. Forest Ecology and Management, 196: 213–225.

Kazeminia A. (2018): Application of remote sensing and GIS in the investigating vegetation coverage. Geospatial Engineering Journal, 9: 75–85.

Kerr J.T., Ostrovsky M. (2003): From space to species: ecological applications for remote sensing. Trends in Ecology & Evolution, 18: 299–305.

Knipling E.B. (1970): Physical and physiological basis for the reflectance of visible and near-infrared radiation from vegetation. Remote Sensing of Environment, 1: 155–159.

Lantschner M.V., Corley J. C. (2015): Spatial pattern of attacks of the invasive woodwasp Sirex noctilio, at landscape and stand scales. PLoS ONE, 10: e0127099.

Liu D., Kelly M., Gong P., Guo Q. (2007): Characterizing spatial-temporal tree mortality patterns associated with a new forest disease. Forest Ecology and Management, 253: 220–231.

Maglione P., Parente C., Vallario A. (2013): Using World-View-2 satellite imagery to support geoscience studies on Phlegraean area. American Journal of Geoscience, 3: 1–12.

Melillos G., Hadjimitsis D.G. (2020): Using simple ratio (SR) vegetation index to detect deep man-made infrastructures in Cyprus. In: Proc. 15th Conf. Detection and Sensing of Mines, Explosive Objects, and Obscured Targets, April 27–May 8, 2020: 114180E.

Menge D., Makobe M., Shomari S. (2013): Effect of environmental conditions on the growth of *Cryptosporiopsis* spp. causing leaf and nut blight on cashew (*Anacardium occidentale* Linn.). Journal of Yeast and Fungal Research, 4: 12–20.

Mohajer M.M. (2006): Forestry and Silviculture. Teheran, University of Tehran Press.

Naji T.A: (2018): Study of vegetation cover distribution using DVI, PVI, WDVI indices with 2D-space plot. Journal of Physics Conference Series, 1003: 012083.

Nepstad D.C., Tohver I.M., Ray D., Moutinho P., Cardinot G. (2007): Mortality of large trees and lianas following experimental drought in an Amazon forest. Ecology, 88: 2259–2269.

Ray S., Das G., Singh J.P., Panigrahy S. (2006): Evaluation of hyperspectral indices for LAI estimation and discrimination of potato crop under different irrigation treatments. International Journal of Remote Sensing, 27: 5373–5387.

Ray S.S., Jain N., Arora R.K., Chavan S., Panigrahy S. (2011): Utility of hyperspectral data for potato late blight disease detection. Journal of the Indian Society of Remote Sensing, 39: 161.

Robinson N.P., Allred B.W., Jones M.O., Moreno A., Kumball J.S., Naugle D.E., Erickson T.A., Richardson A.D. (2017): A dynamic Landsat derived normalized difference vegetation index (NDVI) product for the conterminous United States. Remote Sensing, 9: 863.

Sabety H. (1994): Iran's Forests, Trees and Shrubs. Yazd, Yazd University Press.

Strachinis I., Kazilas C., Karamaouna F., Papanikolaou N.E., Partsinevelos G.K., Milonas P.G. (2015): First record of *Cydalima perspectalis* (Walker, 1859) (Lepidoptera: Crambidae) in Greece. Hellenic Plant Protection Journal, 8: 66–72.

Vani V., Mandla V.R. (2017): Comparative study of NDVI and SAVI vegetation indices in Anantapur district semi-arid areas. International Journal of Civil Engineering & Technology, 8: 287–300.

Whiteside T.G., Boggs G.S., Maier S.W. (2011): Comparing object-based and pixel-based classifications for mapping savannas. International Journal of Applied Earth Observation and Geoinformation, 13: 884–893.

Zhang J., Huang Y., Pu R., González-Moreno P., Yuan L., Wu K., Huang W. (2019): Monitoring plant diseases and pests through remote sensing technology: A review. Computers and Electronics in Agriculture, 165: 104943.

Received: April 4, 2020
Accepted: October 20, 2020